Surface Rheology of Monolayers of Triblock Copolymers of PEO and PPO: Surface Light Scattering Studies at the Air/Water Interface

ARTICLE *in* LANGMUIR · APRIL 2003

Impact Factor: 4.46 · DOI: 10.1021/la034092s

2 AUTHORS, INCLUDING:

Chanjoong Kim
Kent State University
26 PUBLICATIONS **293** CITATIONS

Surface Rheology of Monolayers of Triblock Copolymers of PEO and PPO: Surface Light Scattering Studies at the Air/Water Interface

Chanjoong Kim and Hyuk Yu*

Department of Chemistry, University of Wisconsin−Madison, Madison, Wisconsin 53706

Received January 20, 2003. In Final Form: February 25, 2003

Static and dynamic viscoelastic studies of monolayers of triblock copolymers of poly(ethylene oxide), PEO, and poly(propylene oxide), PPO, are performed at the air/water interface. These copolymers are better known by their trade names of Pluronics and Polaxamers. The technique of surface light scattering (SLS) with the Wilhelmy plate method enables us to probe both static and dynamic viscoelastic properties of the monolayers. The effect of varying the molecular architecture on the surface viscoelastic response is examined with two different copolymers, PEO−PPO−PEO (2.20 kg/mol) and its symmetric counterpart, PPO−PEO−PPO (1.95 kg/mol), over the temperature range 7−32 °C. SLS experiment reveals that the elastic contribution dominates the viscoelastic behavior of both copolymers over the entire temperature range. Further, there is a clear correspondence between the static elasticity and the dynamic viscoelasticity relative to monolayer surface density. When the static elasticity deduced from the surface pressure−surface density isotherm reaches a maximum, the corresponding behavior is observed for the dynamic elasticity and viscosity deduced from SLS.

Introduction

Triblock copolymers of poly(ethylene oxide), PEO, and poly(propylene oxide), PPO, commonly known by one of its trade names, Pluronics, have been used as nonionic surfactants for a variety of applications such as in emulsification and dispersion stabilization. In aqueous solutions, these copolymers form micelles above the critical micelle concentration, and the bulk properties of the resulting colloidal suspensions have been extensively investigated by several groups.[1−5] The surface properties of the adsorbed monolayers of the copolymers have been reported with respect to their structures and static properties,[6−8] whereas their monolayer dynamics have not been hitherto examined.

Monolayer dynamics of adsorbed or spread monolayers can be deduced from the propagation characteristics of spontaneously formed capillary waves on the air/water interface (A/W). Capillary waves propagation is probed by the technique of surface light scattering (SLS) in conjunction with the Wilhelmy plate technique for the simultaneous monitoring of the static surface tension.[9] The capillary waves, induced by thermal fluctuations in the underlying liquid subphase, are modulated by the hydrodynamic motions of a monolayer at the interface. Reductions in the surface tension, and enhanced damping of surface motions have been ascribed to the dilational viscoelastic properties of the monolayers. Several hydrodynamic models were developed to describe the motion of the monolayer-covered interface. The Lucassen−Lucassen−Reynders dispersion relation is selected among different models, and used here to extract viscoelastic parameters from the SLS power spectrum as follows:[10]

$$\eta^2(k - m^*)^2 = \left[\eta(k + m^*) + \frac{\epsilon^* k^2}{i\omega^*}\right]\left[\eta(k + m^*) + \frac{\sigma^* k^2}{i\omega^*} + \frac{g\rho}{i\omega^*} - \frac{\omega^*\rho}{ik}\right] \quad (1)$$

$$m^* = \left(k^{*2} + \frac{i\omega^*\rho}{\eta}\right)^{1/2}, \quad Re(m^*) > 0 \quad (2)$$

$$\omega^* = \omega_0 + i\alpha \quad (3)$$

$$\omega_0 = 2\pi f_s \quad (4)$$

$$\alpha = \pi\Delta f_{s,c} \quad (5)$$

$$\epsilon^* = \epsilon_d + i\omega^*\kappa \quad (6)$$

where k is the spatial wave vector, ϵ_d is the dynamic longitudinal elasticity, which is the sum of the dilational and shear components of the monolayer, κ is the corresponding viscosity, which is the sum of the dilational and shear viscosities of the monolayer, η is the bulk steady shear viscosity of the subphase, ρ is the bulk density of the subphase, σ_d is the dynamic surface tension, and μ is the transverse viscosity of monolayer. The frequency shift, f_s, and the corrected width, $\Delta f_{s,c}$, are determined experimentally by fitting the power spectra with the Lorentzian profiles. The dynamic longitudinal elasticity, ϵ_d, and the dynamic dilational viscosity, κ, are extracted from the dispersion equation with a set of assumptions that include the following: (1) σ_d is the same as the static surface tension, σ_s, which is determined by the Wilhelmy plate

(1) Chu, B. *Langmuir* **1995**, *11*, 414.
(2) Alexandridis, P.; Athanassiou, V.; Fukuda, S.; Hatton, T. A. *Langmuir* **1994**, *10*, 2604.
(3) Alexandridis, P.; Holzwarth, J. F.; Hatton, T. A. *Macromolecules* **1994**, *27*, 2414.
(4) Zhou, Z.; Chu, B. *J. Colloid Interface Sci.* **1988**, *126*, 171.
(5) Prasad, K. N.; Luong, T. T.; Florence, A. T.; Paris, J.; Vaution, C.; Seiller, M.; Puisieux, F. *J. Colloid Interface Sci.* **1979**, *69*, 225.
(6) An, S. W.; Su, T. J.; Thomas, R. K.; Baines, F. L.; Billingham, N. C.; Armes, S. P.; Penfold, J. *J. Phys. Chem. B* **1998**, *102*, 387.
(7) Caseli, L.; Nobre, T. M.; Silva, D. A. K.; Loh, W.; Zaniquelli, M. E. D. *Colloid Surf., B−Biointerfaces* **2001**, *22*, 309.
(8) Munoz, M. G.; Monroy, F.; Ortega, F.; Rubio, R. G.; Langevin, D. *Langmuir* **2000**, *16*, 1083.
(9) Sano, M.; Kawaguchi, M.; Chen, Y. L.; Skarlupka, R. J.; Chang, T.; Zografi, G.; Yu, H. *Rev. Sci. Instrum.* **1986**, *57*, 1158.
(10) Lucassen-Reynders, E. H.; Lucassen, J. *J. Adv. Colloid Interface Sci.* **1969**, *2*, 347.

10.1021/la034092s CCC: $25.00
Published on Web 04/12/2003

method; (2) μ is negligibly small; and (3) ϵ_d and κ are independent of the wave vectors within our accessible range. These assumptions were tested and found to be justified, as reported elsewhere.[11−14]

The critical micelle concentration (cmc) of Pluronics has been found to be rather sensitive to temperature, which is ascribed to the changes in the hydrophilicity of the ethylene oxide moiety with temperature.[3] The surface viscoelasticity of polymer monolayers is established to be highly correlated with the hydrophilicity of polymer backbones, such as in polyethers, and/or that of the pendant group in vinyl polymers.[13,15] Our objective here is to seek a corresponding temperature sensitivity of the surface viscoelasticity of these copolymers.

Experimental Section

Materials and Monolayer Preparation. Two kinds of Pluronics, L44 and 10R5, were obtained from BASF. L44 has the structure $(EO)_{10}-(PO)_{22}-(EO)_{10}$ with an overall molecular weight of 2.20 kg/mol, and 10R5 has the structure $(PO)_8-(EO)_{22}-(PO)_8$ with a corresponding molecular weight of 1.95 kg/mol, where EO represents a $-CH_2-CH_2-O-$ unit and PO represents a $-CH_2-CH(CH_3)-O-$ unit. These samples were used without further purification. HPLC grade chloroform was used as the spreading solvent. Pluronics solutions with concentrations of 0.02−0.04 g/L were prepared in chloroform. Deionized water without specific buffering was used as the subphase. The deionized water was the house-deionized water that was further purified by a Millipore-Q2 system with an initial resistivity of greater than 17 MΩ. The monolayer surface mass density, henceforth called surface concentration, Γ, for short, for all measurements was varied by the successive addition method with a substantial waiting period to reach apparent equilibrium for each addition (see below).

Surface Pressure and Static Surface Elasticity. Experiments were carried out in a Teflon trough with a size of 307 cm^2, which was housed in a chamber made of Plexiglass and insulated with Styrofoam for humidity and temperature control, which was obtained by circulating thermostated ethylene glycol around the chamber from a Lauda bath (Lauda RM6).

The relative humidity within the chamber was kept at 98% or above during all measurements. The temperature inside the chamber was monitored and maintained to within ±0.2 °C. The surface tensions of the bare and monolayer-covered surface were determined by the Wilhelmy technique using a sandblasted platinum plate (26.9 mm × 10.3 mm × 0.1 mm).

The trough and platinum plate were soaked in H_2SO_4 mixed with Nochromix overnight and washed thoroughly with deionized water. The surface tension, γ, was observed with an electrobalance (Cahn Instrument, 2000). The equilibrium surface tension was determined after the time dependence, $d\gamma/dt$, was less than approximately 10^{-3} mN/m·min.

The static elasticity, ϵ_s, was calculated from the surface pressure (Π)−surface concentration (Γ) isotherm by

$$\epsilon_s = \Gamma\left(\frac{\partial \Pi}{\partial \Gamma}\right)_T \tag{7}$$

which is the surface analogue of the bulk modulus, $B \equiv \rho(\partial P/\partial \rho)_T$, where P is the isotropic pressure and ρ is the density.

Surface Light Scattering. The surface light scattering experimental setup has been described in detail elsewhere.[9] Thus, we describe it here only briefly to highlight some recent changes. Light from an He−Ne laser (7 mW, 632.8 nm, Melles Griot 05LHP 171) is incident at an angle of 64.3° normal to the surface. The principal feature of the apparatus is the use of a transmission diffraction grating to select a specific wave vector and provide a reproducible source for heterodyne beating which is generated by the light scattered by surface ripples and the diffraction beam reflected from the air/water interface. The desired diffraction order of the beam is guided to a photomultiplier tube (PMT) by a mirror. The current from the PMT is successively passed through a voltage divider and high-pass filter amplifier (Ithaco 4302 dual filter) with a cutoff frequency of 800 Hz and 10× amplification. The signal is then sent to a PC via an oscilloscope (Tektronix TDS210) and averaged, usually for 512 counts, after the fast Fourier transform (FFT). The trough chamber is hung by four sets of steel springs with damping sponges from a steel frame structure to isolate mechanical vibration. In this work the fourth, fifth, and sixth order diffraction spots were used to define the scattering angle. The corresponding wave vectors were k = 266, 328, and 389 cm^{-1}, respectively. In Figure 1 we display examples of the fourth, fifth, and sixth order power spectra.

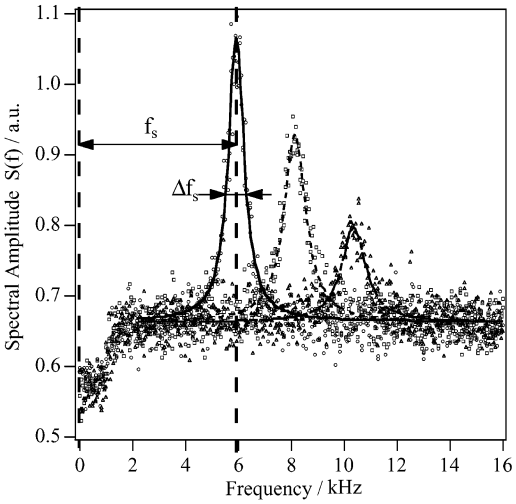

Figure 1. Fourth (○), fifth (□), and sixth (△) orders of the power spectra, which were fit with Lorentzian functions.

Results and Discussion

Static Properties. Surface concentration, Γ, is calculated with the assumption that all the polymers spread on the surface remain there without desorption into the subphase. Figure 2 displays (a) Π−Γ isotherms and (b) the static surface elasticity, ϵ_s, as a function of Γ for L44 (PEO−PPO−PEO) at three different temperatures. It appears that the Π and ϵ_s values at 9 °C prior to the maximum static elasticity, $\epsilon_{s,max}$, are marginally higher than those at 23 and 30 °C. Also, the values of the threshold surface concentration, Γ*, where $\epsilon_{s,max}$ is attained, seemingly increase with temperature although the same trend cannot be said to persist for the temperature interval of 23−30 °C. Stated otherwise, the trend indicates that the nominal area per unit mass ($A^*_{nominal} = 1/\Gamma^*$) decreases with increasing temperature. In terms of earlier studies with PEO−PS diblock copolymers and PEO homopolymers,[16,17] we plausibly estimated the fully covered monolayer state to be at Γ*. If so, the temperature dependence of Γ* may qualitatively be explained as follows. The amount of the PEO block submerging into the subphase increases with increasing temperature because of increasing solubility and/or decreasing surface activity of the PEO block. An alternative explanation, but also consistent with the experiment, can be made that the PEO blocks get less hydrated with increasing temperature. Alexandridis et al.[3] proposed that the temperature dependence of the critical micelle concentration of these

(11) Crilly, J. F.; Earnshaw, J. C. *Biophys. J.* **1983**, *41*, 211.
(12) Crilly, J. F.; Earnshaw, J. C. *Biophys. J.* **1983**, *41*, 197.
(13) Yoo, K. H.; Yu, H. *Macromolecules* **1989**, *22*, 4019.
(14) Langevin, D. *J. Colloid Interface Sci.* **1981**, *80*, 412.
(15) Esker, A. R.; Zhang, L. H.; Olsen, C. E.; No, K.; Yu, H. *Langmuir* **1999**, *15*, 1716.
(16) Sauer, B. B.; Kawaguchi, M.; Yu, H. *Macromolecules* **1987**, *20*, 2732.
(17) Sauer, B. B.; Yu, H.; Tien, C. F.; Hager, D. F. *Macromolecules* **1987**, *20*, 393.

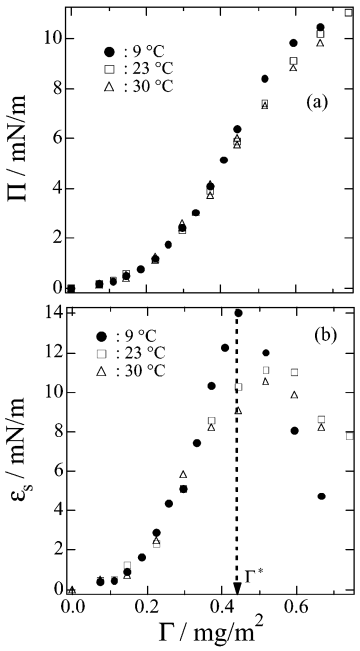

Figure 2. Π−Γ isotherms (a) and ϵ_s−Γ (b) for L44 on the air/water interface at various temperatures: 9 °C (●); 23 °C (□); 30 °C (△). Γ* indicates the concentration where the static elasticity at 9 °C reaches the maximum value.

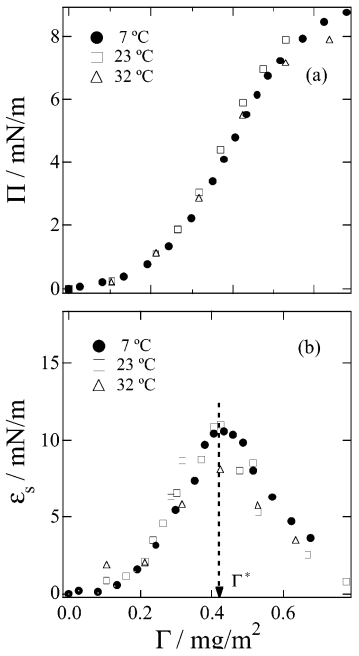

Figure 3. Π−Γ isotherms (a) and ϵ_s−Γ (b) for 10R5 on the air/water interface at various temperatures: 7 °C (●); 23 °C (□); 32 °C (△). Γ* indicates the concentration where the static elasticities of all three temperatures reach their maxima.

triblock copolymers can arise from less hydration of the PEO block and/or increasing hydrophobicity of the PPO block, that is, polymer blocks losing associated water molecules with increasing temperature due to conformational changes of polymer in the solution. A similar argument was provided by Shuler and Zisman[18] that the chain conformation on the air/water interface begins to change from the all trans-conformation, which has 20 Å^2/monomer as a nonhydrated area per monomeric unit and 28 Å^2/monomer as a hydrated area, to the cis-conformation, which has 16 Å^2/monomer as a nonhydrated area when the surface film gets compressed to values less than 20 Å^2/monomer. However, the threshold surface concentration of L44 at 9 °C, Γ* = 0.4 mg/m^2, corresponds to A^*_{nominal} of 17 Å^2/monomer, and Γ* at 23 and 30 °C are about 0.5 mg/m^2, corresponding to A^*_{nominal} of 14 Å^2/monomer. The conformational change with changing area per monomer may be possible, but A^*_{nominal} values at higher temperatures are even smaller than the nonhydrated area per monomeric unit, 20 Å^2/monomer. More recent experimental data[8] are used to infer that the PEO blocks form brushes under the surface at higher concentrations, which is in accord with our previous proposal that some of the end-chain PEO blocks penetrate into the subphase.

Next, we turn to the results obtained with the other sample, 10R5 (PPO−PEO−PPO). Figure 3 shows the analogous plots of Figure 2 for 10R5: (a) Π−Γ isotherms and (b) the static surface elasticity, ϵ_s, as a function of Γ at three different temperatures. Relative to the Π−Γ isotherms and the threshold surface concentration Γ* (equaling 0.4 mg/cm^2), there is no temperature dependence, which is in complete contrast to the results for L44; for 10R5 no temperature dependence can be discerned within experimental uncertainties. A qualitative interpretation of this contrasting behavior is offered as follows. Unlike the case with L44, where PEO blocks in both ends of PPO are conformationally free to respond to temperature changes, the PEO block in the middle of the PPO−PEO−PPO triblock (10R5) is conformationally pinned by PPO blocks.

Dynamic Viscoelastic Properties. As laid out in the Introduction, we extract two viscoelastic parameters, dilational elasticity, ϵ_d, and the corresponding viscosity, κ, by SLS from the two observables, a measure of capillary wave propagation rate, f_s, and that of the wave damping, $\Delta f_{s,c}$. To compare the dynamics of different monolayers, we employ a method of the corresponding wave propagation characteristics with a choice of a reference interface. It is convenient to construct a reference polar plot by specifying the propagation parameters ($f_{s:eq}$ and $\Delta f_{s,c:eq}$, where eq stands for equivalent) computed for different values of the dilational elasticity.[19] Such a polar plot is constructed with the specified values of dynamic surface tension, σ_d, transverse viscosity, μ, and the subphase characteristics of density, ρ, and shear viscosity, η, for a given scattering wave vector, k. Once the reference interface is specified, all monolayer dynamics with known ϵ_d and κ can be compared by computing the corresponding capillary wave propagation parameters. The method is detailed elsewhere;[19] hence, we dwell no more on the exposition of the reference polar plot. Figure 4 shows the damping coefficient, $\Delta f_{s,c:eq}$, versus the propagation frequency, $f_{s:eq}$, with varying ϵ_d and κ at the specified values of σ_d, μ, ρ, η, and k corresponding to the reference state chosen. This graph shows two poles: (0, 0) and (∞, ∞) for (ϵ_d, κ). The polar plot has a unique feature relative to resolution. As the surface viscoelasticity increases, the spacing between grids decreases, resulting in broadening of imprecision for the viscoelastic parameters. Thus, exact specifications of viscoelastic parameters are difficult to obtain when ϵ_d and κ exceed 20 mN/m and 3 × 10^{-4} mN·s/m, respectively. Esker et al.[19] compared two classes of polymers: hydrophilic and hydrophobic polymers. The hydrophilic class shows elasticity-dominant behavior while hydrophobic polymers show viscosity-dominant behavior.

(18) Shuler, R. L.; Zisman, W. A. *J. Phys. Chem.* **1970**, *74*, 1523.

(19) Esker, A. R.; Zhang, L. H.; Sauer, B. B.; Lee, W.; Yu, H. *Colloid Surf., A—Physicochem. Eng. Aspects* **2000**, *171*, 131.

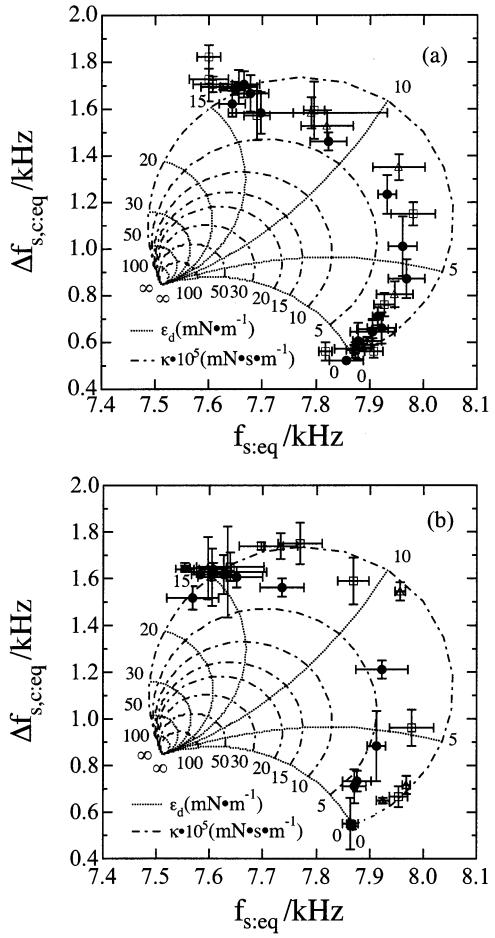

Figure 4. Polar plot for L44 (a) at various temperatures [9 °C (●); 23 °C (□); 30 °C (△)] and that for 10R5 (b) at similar temperatures [7 °C (●); 23 °C (□); 32 °C (△)]. $\Delta f_{s,c:eq}$ and $f_{s:eq}$ are calculated on the basis of the reference state that $k_{ref} = 324.3$ cm^{-1}, $\eta_{ref} = 0.894$ cP, $\rho_{ref} = 0.997$ g/cm^3, $\sigma_{d,ref} = 71.79$ mN/m, and $\mu_{ref} = 0$ mN·s/m (water at 25 °C). The solid curves correspond to constant value of ϵ_d while the dashed−dot loops show $\kappa \times 10^5$. The values represent averages over three wave vectors.

The triblock copolymers under study here pose an intriguing question by virtue of their architectural difference in the hydrophilic EO/hydrophobic PO moieties. The case of L44 (with PEO−PPO−PEO) has a greater amount of hydrophilic PEO blocks that are conformationally freer than those in 10R5 (with PPO−PEO−PPO), where a PEO block is also conformationally pinned by the PPO blocks.

The polar plots of L44 at 9, 23, and 30 °C are shown in Figure 4a while those of 10R5 at 7, 23, and 32 °C are displayed in part b. Each point was averaged over the values obtained from the fourth, fifth, and sixth diffraction orders. The overall behavior of the monolayer shows viscoelastic behavior dominated by the elastic component. Marginally, lower temperature conditions show higher viscosity. There are a few studies about the temperature dependence of the surface dilational viscosity of polymers. Monroy et al.[20] showed that the dilational viscosity of poly(vinyl acetate) increases with temperature below a kind of transition temperature and then decreases in the Arrhenius form at higher temperatures. Our temperature range may be higher than a corresponding temperature for these triblock copolymers.

(20) Monroy, F.; Ortega, F.; Rubio, R. G. *Eur. Phys. J. B* **2000**, *13*, 745.

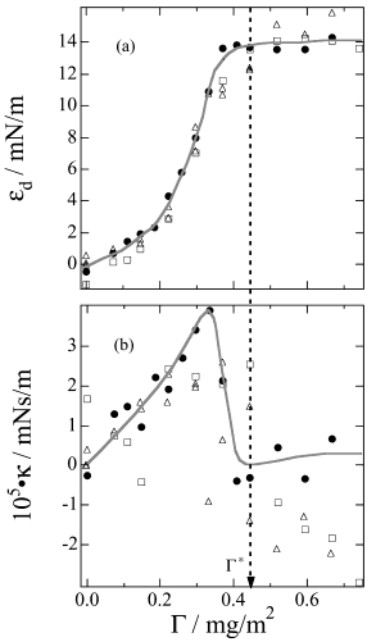

Figure 5. ϵ_d−Γ (a) and κ−Γ (b) for L44 on water at various temperatures: 9 °C (●); 23 °C (□); 30 °C (△). The hydrodynamic values represent averages over three wave vectors. Solid lines are guides for the trends at 9 °C. Error bars are omitted for clarity. Γ^* comes from Figure 2b.

The viscoelastic behavior of L44 (PEO−PPO−PEO) at 9 °C is somewhat different than those at higher temperatures. At 9 °C, the dynamic dilational elasticity, ϵ_d (Figure 5a, ●), reaches an asymptotic value (∼14 mN/m^2) and the corresponding viscosity, κ (Figure 5b, ●), drops abruptly to 0 mN·s/m around the threshold concentration ($\Gamma^* \approx 0.4$ mg/m^2), where the static elasticity exhibits its maximum value, whereas in the cases of 23 and 30 °C (Figure 5a, □ and △), the dynamic dilational elasticity reaches an asymptotic value (∼15 mN/m^2) and the dilational viscosity drops to -1×10^{-5} mN·s/m around $\Gamma^* \approx 0.5$ mg/m^2, which is higher than that at 9 °C. There is no abrupt drop of the dilational viscosities at 23 and 30 °C, in sharp contrast to the viscosity behavior at 9 °C, and the maximum viscosity value (∼ 2×10^{-5} mN·s/m) at 23 and 30 °C is significantly lower than the corresponding value (∼ 4×10^{-5} mN·s/m) at 9 °C.

Figure 6 shows ϵ_d−Γ (a) and κ−Γ (b) plots for 10R5 (PPO−PEO−PPO). Dynamic dilational elasticities, ϵ_d, at different temperatures reach their asymptotes at the same surface concentration (∼0.5 mg/m^2), which is a little bit higher than Γ^* (0.4 mg/m^2) for L44 (PEO−PPO−PEO). The corresponding viscosities, κ, at three different temperatures reach the minima at the same value of Γ^* where the static elasticities obtain their maximum values, while the viscosity maxima and concentrations are quite different for the three temperatures. The maximum dilational viscosities of these triblock copolymers decrease with increasing temperature while the values of the maximum dynamic elasticities are almost temperature insensitive within our range of observable wave vectors.

Negative values of the dilational viscosities might be a consequence of an improper assumption, such as the transverse viscosity is zero. However, the negative values of the dilational viscosities together with nonzero transverse viscosity have been observed and discussed extensively for various PEO-containing systems and other

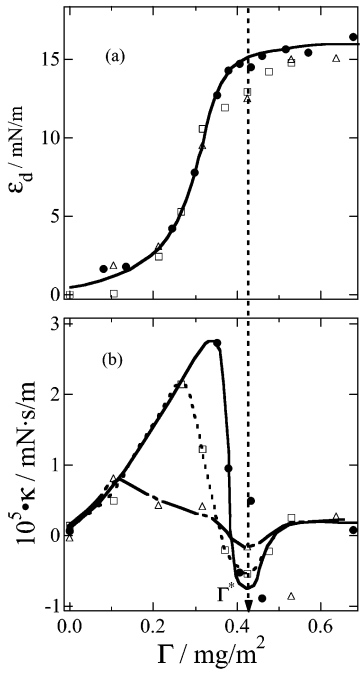

Figure 6. ϵ_d−Γ (a) and κ−Γ (b) for 10R5 on water at various temperatures: 7 °C (●); 23 °C (□); 32 °C (△). The hydrodynamic values represent averages over three wave vectors. Solid lines are guides for the trends at 7 °C. The dotted line highlights the trend for κ at 23 °C, and the line−dotted line does the same for 32 °C. Error bars are omitted for clarity. Γ* comes from Figure 3b.

polymers by the groups of Earnshaw and Richards.[21−24] They did not assume the transverse viscosity to be zero as we do. Whereupon it was extracted from the curve fitting of the spectral profiles in time domain with more variables than we use but still they obtained negative dilational viscosities. We propose the following as an explanation. As the PEO blocks penetrate into the subphase with increasing surface concentration, the Lucassen−Lucassen−Reynders dispersion equation no longer holds true, mainly because the interface is not restricted to monolayers after the collapse of polymers, and there are interactions among collapsed loops and tails under the air/water interface. L44 shows larger negative values of dilational viscosities than 10R5. While the PEO blocks in L44 are likely to form loops and tails after collapse, the PEO block in 10R5 is not due to the pinning restriction imposed by the PPO blocks. Any accounting of the interactions between collapsed polymer chains on the interface was not included in the dispersion equation.

Conclusions

We investigated surface viscoelastic behaviors of two types of triblock copolymers of PEO and PPO at the air/water interface over a limited temperature range of 7∼32 °C with the techniques of the Wilhelmy plate method and the surface light scattering method. On the basis of our experiment results, the overall viscoelastic behavior of these triblock copolymers is dominated by the elastic contributions. In terms of the chain conformations, we propose a simple model. After reaching the threshold surface concentration where the static elasticity reaches the maximum, these triblock copolymers collapse into the subphase and form hydrated brushes. These anchored brushes may be responsible for the result that the surface viscosities become negative at Γ values >Γ*. A distinctive difference between two types of polymers, L44 (PEO−PPO−PEO) and 10R5 (PPO−PEO−PPO), is the temperature dependence of Γ*, where both the static elasticity and dilational viscosity show some yet to be fully defined "transitions". Γ* of L44 increases with increasing temperature while that of 10R5 does not change with temperature.

Acknowledgment. This work was partially supported by the Eastman Kodak Professorship and an NSF grant (DMR0084301) awarded to H.Y. We are grateful for helpful discussions with our colleagues Thorsteinn Adalsteinsson and Weiguo Cheng.

LA034092S

(21) Peace, S. K.; Richards, R. W.; Williams, N. *Langmuir* **1988**, *4*, 667.
(22) Richards, R. W.; Taylor, M. R. *J. Chem. Soc., Faraday Trans.* **1996**, *92*, 601.
(23) Richards, R. W.; Taylor, M. R. *Macromolecules* **1997**, *30*, 3892.
(24) Earnshaw, J. C.; McCoo, E. *Langmuir* **1995**, *11*, 1087.